Chemically Sensitive Surface Acoustic Wave Devices Employing a Self-Assembled Composite Monolayer Film: Molecular Specificity and Effects Due to Self-Assembled Monolayer Adsorption Time and Gold Surface Morphology

Ross C. Thomas,† Huey C. Yang,‡ Chris R. DiRubio,§ Antonio J. Ricco,*,† and Richard M. Crooks*,‡

Microsensor Research and Development and Surface and Interface Sciences Department, Sandia National Laboratories, Albuquerque, New Mexico 87185-1425, and Department of Chemistry, Texas A&M University, College Station, Texas 77843-3255

Received June 21, 1995. In Final Form: January 2, 1996⊗

The selectivity, sensitivity, and reproducibility of SAW chemical sensors functionalized with a carboxylate-coordinated Cu^{2+}-terminated surface are examined in relation to the interfacial properties of these organomercaptan self-assembled monolayer (SAM) films, prepared from the solution phase for adsorption times of 36, 84, or 180 h on Au surfaces having variable, controlled grain sizes. SAM adsorption time and the grain size of the Au film can dramatically affect the response to adsorption from the vapor phase onto the composite monolayer-modified SAW device. It is proposed that the varied response results from differences in molecular packing and, particularly, in the ordering of the end groups of the monolayer film that provide the chemically sensitive interface. These studies provide an important step toward reliably fabricating chemical sensors that respond to specific classes of organic analytes.

Introduction

Chemically sensitive surface acoustic wave (SAW) devices provide a basis to design sensors that respond to specific classes of organic analytes.[1] While custom-designed and synthesized molecular recognition sites are an appealing answer to chemical specificity, the difficult, time-intensive nature of this approach, coupled with the very large number of molecules for which chemical sensors are sought and the difficulty of dealing with nonspecific adsorption, may mean that custom guest−host complexes will ultimately find application only in a small fraction of successful chemical sensor systems. An alternate approach is to relax selectivity requirements significantly, though not completely, and use arrays of two or more devices, relying on the "fingerprint" offered by the pattern of responses to identify a particular analyte.[2−15]

To rationally design chemically sensitive interfaces of moderate selectivity, then, an appealing approach is to make use of known reversible bulk-phase interactions between the analyte and functional moieties that can be incorporated into a thin film.[16,17] Composite self-assembled monolayer (SAM) films that employ organomercaptan molecules have the potential to provide a simple methodology for fabricating such chemically active vapor/solid interfaces that respond reversibly and reproducibly to a wide spectrum of organic analytes. For example, SAMs prepared using 0.5−10 mM ethanolic solutions of an appropriate *n*-alkanethiol for formation times ranging from 1 to 100 h produce monolayers with similar average properties (i.e., surface coverage, structure, and orientation).[18] Furthermore, several research groups, including our own, have extensively studied the chemical reactivity of organomercaptan monolayers, as well as the interactions of these films with vapor-, liquid-, and solid-phase reactants, which provide detailed information about the wetting properties,[18] adhesion forces,[19,20] and molecular interactions[21−23] of the SAM terminal groups.

* Authors to whom correspondence should be addressed.
† Microsensor Research and Development Department, Sandia National Laboratories.
‡ Department of Chemistry, Texas A&M University.
§ Surface and Interface Sciences Department, Sandia National Laboratories.
⊗ Abstract published in *Advance ACS Abstracts,* April 1, 1996.

(1) (a) Hughes, R. C.; Ricco, A. J.; Butler, M. A.; Martin, S. J. *Science* **1991**, *254*, 74. (b) Grate, J. W.; Martin, S. J.; White, R. M. *Anal. Chem.* **1993**, *65*, 940A, 987A. (c) Ward, M. D.; Buttry, D. A. *Science* **1990**, *249*, 1000. (d) Ballantine, Jr., D. S.; Wohltjen, H. *Anal. Chem.* **1989**, *61*, 704A.
(2) Ballantine, D. S., Jr.; Rose, S. L.; Grate, J. W.; Wohltjen, H. *Anal. Chem.* **1986**, *58*, 3058.
(3) Bott, B.; Jones, T. A. *Sens. Actuators* **1986**, *9*, 19.
(4) Carey, W. P.; Beebe, K. R.; Kowalski, B. R. *Anal. Chem.* **1987**, *59*, 1529.
(5) Stetter, J. R.; Findlay, M. W.; Maclay, G. J. *Sens. Actuators, B* **1990**, 1, 43.
(6) Horner, G.; Hierold, Chr. *Sens. Actuators, B* **1990**, *2*, 173.
(7) Schierbaum, K. D.; Weimar, U.; Göpel, W. *Sens. and Actuators, B* **1990**, *2*, 71.
(8) Müller, R. *Sens. Actuators, B* **1991**, *4*, 35.
(9) Nakamoto, T.; Fukuda, A.; Moriizumi, T.; Asakura, Y. *Sens. Actuators, B* **1991**, *3*, 221.
(10) Winquist, F.; Sundgren, H.; Hedborg, E.; Spetz, A.; Lundström, I. *Sens. Actuators, B* **1992**, *6*, 157.
(11) Shurmer, H. V.; Gardner, J. W. *Sens. Actuators, B* **1992**, *8*, 1.
(12) Davide, F. A. M.; D'Amico, A. *Sens. Actuators, A* **1992**, *32*, 507.
(13) Schmautz, A. *Sens. Actuators, B* **1992**, *6*, 38.
(14) Zellers, E. T.; Patrash, S. J. *Anal. Chem.* **1992**, *65*, 2055.
(15) Ricco, A. J.; Xu, C.; Crooks, R. M.; Allred, R. E. In *Interfacial Design and Chemical Sensing*; ACS Symposium Series No. 561; American Chemical Society: Washington, DC, 1994; Chapter 23, pp 264−279.
(16) Kepley, L. K.; Crooks, R. M.; Ricco, A. J. *Anal. Chem.* **1992**, *64*, 3191.
(17) (a) Ebersole, R. C.; Miller, J. A.; Moran, J. R.; Ward, M. D. *J. Am. Chem. Soc.* **1990**, *112*, 3239. (b) Mirken, C. A.; Wrighton, M. S. *J. Am. Chem. Soc.* **1990**, *112*, 8596. (c) Steinberg, S.; Rubinstein, I. *Langmuir* **1992**, *8*, 1183.
(18) (a) Nuzzo, R. G.; Allara, D. L. *J. Am. Chem. Soc.* **1983**, *105*, 4481. Bain, C. D.; Troughton, E. B.; Tao, Y.-T.; Evall, J.; Whitesides, G. M.; Nuzzo, R. G. *J. Am. Chem. Soc.* **1989**, *111*, 321, and references therein. (b) Dubois, L. H.; Nuzzo, R. G. *Annu. Rev. Phys. Chem.* **1992**, *43*, 437 and references therein.
(19) Thomas, R. C.; Houston, J. E.; Crooks, R. M.; Kim, T.; Michalske, T. A. *J. Am. Chem. Soc.* **1995**, *117*, 3830.
(20) Frisbie, C. D.; Rozsnayai, L. F.; Noy, A.; Wrighton, M. S.; Lieber, C. M. *Science* **1994**, *266*, 771.
(21) Thomas, R. C.; Tangyunyong, P.; Houston, J. E.; Michalske, T. A.; Crooks, R. M. *J. Phys. Chem.* **1994**, *98*, 4493.
(22) (a) Sun, L.; Thomas, R. C.; Crooks, R. M.; Ricco, A. J. *J. Am. Chem. Soc.* **1991**, *113*, 8550. (b) Sun, L.; Kepley, L. J.; Crooks, R. M. *Langmuir* **1992**, *8*, 2101. (c) Sun, L.; Crooks, R. M.; Ricco, A. J. *Langmuir* **1993**, *9*, 1775.
(23) Duevel, R. V.; Corn, R. M. *Anal. Chem* **1992**, *64*, 337.

S0743-7463(95)00498-7 CCC: $12.00 © 1996 American Chemical Society

In most cases, SAM films are formed onto Au surfaces that are thermally or electron-beam evaporated onto Ti- or Cr-primed Si(100) substrates, but they are also commonly formed on Au-covered glass, quartz, or mica surfaces, as well as single-crystal Au(111) substrates.[18] Although the wide range of substrate materials and deposition conditions produce Au films having different grain sizes and surface roughnesses, SAM films having similar macroscopic properties are nevertheless formed. The ordering of the S head group onto the primarily (111) crystallite orientation found to predominate for all of these Au surfaces, along with the densely-packed self-assembly of the alkane portion of the organomercaptan molecules, most likely accounts for the consistent characteristics of the Au-supported SAMs.

Recent studies show, however, that subtle effects (e.g., number of defects) within a SAM film may result from differences in the microstructure, presumably associated with grain boundaries, of the underlying Au film.[24,25] In these reports, however, it is not clear that the authors invariably used the same monolayer adsorption time, a parameter that could also affect the quality of the SAM film. Several reports have previously shown that a specific defect structure results for SAM films prepared using solution-phase adsorption times of 24−48 h.[26,27] Moreover, a recent STM study clearly illustrates that it takes many days for the Au surface to reorganize in the presence of thiols and many days for self-assembly to be complete under certain conditions.[28]

We use SAW devices as physical transduction platforms for chemical sensors and interfacial chemical studies because of their extreme sensitivity to surface adsorbates.[1] For example, we measure a surface mass detection limit of ca. 100 pg/cm^2 because the acoustic energy is largely confined to within one wavelength of the surface, coupled with the fact that the frequency stability of our 97-MHz SAW oscillator circuit is about 1 Hz over time intervals exceeding 1 min.[29] In many cases, it is appropriate to assume that the velocity of the SAW is perturbed in direct proportion to the surface mass loading of the device, which is measured as a change in frequency when the device is used as the feedback element of an oscillator circuit.[29] When they do occur, changes in the mechanical properties of a selective coating interacting with a vapor-phase analyte often result in attenuation of the acoustic wave, in addition to their influence on the SAW velocity (and hence oscillation frequency).[30,31]

We recently demonstrated that a SAW sensor covered by an organomercaptan self-assembled monolayer film[18] having a carboxylate-coordinated Cu^{2+} end group can be used to reversibly detect organophosphonates (Figure 1).[16] The original selection of Cu^{2+} was based on its reported ability to function as a phosphonate hydrolysis catalyst.[32] In this report, we compare the SAW response from a carboxylate coordinated Cu^{2+}-terminated SAM to that from a methyl-terminated SAM, as these films interact with a vapor-phase organophosphonate analyte as well as the vapors of a number of common organic solvents. We also examine in detail the effects of solution-phase SAM adsorption time and the grain size of the supporting Au surface.

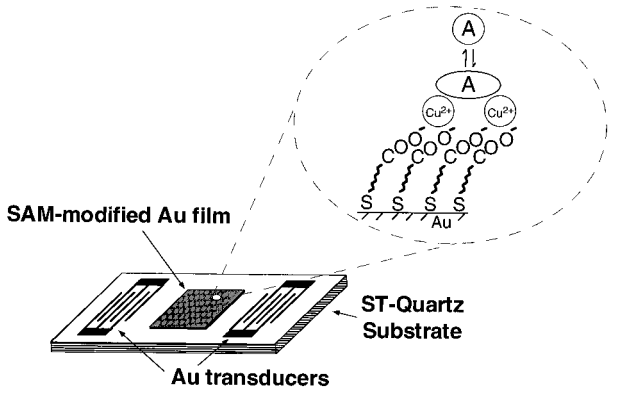

Figure 1. Schematic diagram of a self-assembled composite monolayer-modified chemically sensitive SAW device. The $(COO^-)_2/Cu^{2+}$-terminated interface depicted here displays significant selectivity, in addition to reversibility and durability, for detecting organophosphonate nerve-agent simulants.

Experimental Details

Chemicals. The following chemicals were used as received: diisopropyl methylphosphonate, DIMP (98%, Alfa); absolute ethanol (Aaper alcohol); 11-mercaptoundecanoic acid, MUA (98%) and $Cu(ClO_4)_2 \cdot 6H_2O$ (both from Aldrich); acetone, isooctane, 1-propanol, trichloroethylene (TCE), sulfuric acid, and 30% hydrogen peroxide (all from Fisher). Water was purified by double distillation.

Au Substrate Preparation. Au films, 100 nm thick, were electron-beam evaporated onto the active surface region of clean ST-quartz SAW devices. No Cr or Ti adhesion layer was used since both of these metals are known to diffuse through Au films, which could potentially interfere with comparisons between composite SAM films formed for different lengths of time and on Au surfaces having variable grain sizes. The substrate temperature was maintained at either room temperature or 100 °C during the deposition. The pressure during the Au evaporation was $(1-2) \times 10^{-6}$ mmHg. Au films evaporated onto 100 °C substrates were annealed at either 150 or 250 °C for 2 h in the same deposition chamber, following backfilling with N_2 to a pressure of 1−5 mmHg.

Composite Monolayer Formation. Composite monolayer films were prepared immediately upon removal of the SAW devices having newly deposited Au films from the evaporation chamber by (1) immersing the substrates in a 0.5 mM ethanolic solution of MUA for 36, 84, or 180 h, (2) thoroughly rinsing with ethanol, deionized water, and ethanol again, (3) immersing these carboxylic acid-terminated SAM films in a 2 mM ethanolic solution of $Cu(ClO_4)_2 \cdot 6H_2O$ for 10 min, and (4) thoroughly rinsing the composite monolayer film with ethanol before drying with N_2. Previous Fourier transform infrared external reflectance spectroscopy and X-ray photoelectron spectroscopy measurements of similarly prepared composite monolayer films have confirmed the formation of the $(COO^-)_2/Cu^{2+}$ interface.[16]

Au Surface Characterization. A Nanoscope "StandAlone" atomic force microscope (Digital Instruments, Santa Barbara, CA) was used to analyze the grain size of the SAM-modified Au film after the SAW measurements. The AFM measurements were done in air using commercially available Si_3N_4 microfabricated cantilevers having ∼100 nm probe radii and ∼0.01 N/m spring constants. Data processing consisted of removing the same periodic noise observed in all of the scans and setting the height scale at 30 nm to facilitate direct comparison between the images. Electrochemical surface roughness measurements were carried out in a single-compartment, three-electrode glass cell containing a Ag/AgCl (saturated KCl) reference electrode and a

(24) Guo, L.-H.; Facci, J. S.; McLendon, G.; Mosher, R. *Langmuir* **1994**, *10*, 4588.
(25) Creager, S. E.; Hockett, L. A.; Rowe, G. K. *Langmuir* **1992**, *8*, 854.
(26) Fenter, P.; Eisenberger, P.; Liang, K. S. *Phys. Rev. Lett.* **1993**, *70*, 2447.
(27) Camillone, N., III; Chidsey, C. E. D.; Eisenberger, P.; Fenter, P.; Li, J.; Liang, K. S.; Liu, G.-Y.; Scoles, G. *J. Phys. Chem.* **1993**, *99*, 744.
(28) Poirier, G. E.; Tarlov, M. J. *J. Phys. Chem.* **1995**, *99*, 10960.
(29) Ricco, A. J.; Frye, G. C.; Martin, S. J. *Langmuir* **1989** *5*, 273.
(30) (a) Martin, S. J.; Frye, G. C. *Poc. 1991 Ultrasonics Symposium*; IEEE: New York, 1991; pp 393−398. (b) Martin, S. J.; Frye, G. C.; Senturia, S. D. *Anal. Chem.* **1994**, *66*, 2201. (c) Martin, S. J.; Frye, G. C. *Appl. Phys. Lett.* **1990**, *57*, 1867. (d) Martin, S. J.; Ricco, A. J. *Sens. Actuators* **1990**, *A22*, 712.
(31) Thomas, R. C.; Sun, L.; Crooks, R. M.; Ricco, A. J. *Langmuir* **1991**, *7*, 620.
(32) Wagner-Jauregg, T.; Hackley, B. E., Jr.; Lies, T. A.; Owens, O. O.; Proper, R. J. *J. Am. Chem. Soc.* **1955**, *77*, 922.

Pt counter electrode. Bare Au films, which were evaporated onto ST-cut quartz and had approximately the same grain sizes as those used in the SAW measurements, were used as the working electrodes. The active area (1.23 cm^2) was reproducibly defined by pressing a Viton O-ring between the Au surface and the glass cell. The electrochemical measurements were performed with a Pine Instruments Model AFRDE4 bipotentiostat, and data were recorded on a Kipp and Zonen Model BD-90 X-Y recorder. Cyclic voltammograms were acquired by oxidizing/reducing the Au surfaces between 0.2 and 1.4 V at a rate of 0.1 V/s in 0.24 M $HClO_4$. The surface roughness factor was estimated by integrating the amount of current required to reduce the Au oxide peak and dividing this number by the calculated value of the amount of charge necessary to oxidize an atomically flat Au(111) surface (1.4×10^{15} Au atoms/cm^2)[33] having the same active area.[34]

SAW Experiments. SAW measurements were performed immediately following composite SAM film formation to minimize "aging" effects. Approximately 1−2 h were required to stabilize the SAW device under ultrahigh purity N_2 before taking the first measurements. SAW devices (97 MHz) on ST-quartz with Ti-primed Au transducers were designed and fabricated at Sandia National Laboratories.[35] The SAW measurements were performed according to previously described procedures.[22a,29,31] Adsorption/desorption isotherms for newly prepared composite monolayer films exposed to acetone, DIMP, isooctane, 1-propanol, trichloroethylene, toluene, and water were measured over vapor-phase concentrations ranging from 0%- to 50%-of-saturation in a N_2 carrier gas stream at 21.6 ± 0.1 °C using a computer-controlled flow system described elsewhere.[36] One DIMP isotherm was taken before and after exposure to the set of all other organic solvents. Isotherms were obtained over a total of 4 h for each analyte (2 h each for adsorption and desorption).

If the SAW velocity is perturbed only by mass loading variations, the change in frequency, Δf, is related to the change in adsorbed mass per area, $\Delta(m/A)$, by eq 1[35]

$$\Delta f/f_o = -\kappa c_m f_o \Delta(m/A) \quad (1)$$

where c_m is the mass sensitivity (1.33 cm^2/g-MHz for ST-quartz), f_o is the unperturbed oscillator frequency (97 MHz), and κ is the fraction of the center-to-center distance between the transducers covered by the Au film; its present value is 0.7. Thus, the active region of the SAW device is covered by 70% Au of controlled grain size and 10% Au/Ti transducer fingers that are small-grain-size Au,[37] and the remaining 20% is bare quartz.

In addition to frequency changes, the insertion loss was also recorded during all SAW experiments. Changes in this quantity are directly proportional to changes in the attenuation of the surface acoustic wave, α, which is typically normalized by division by the wavenumber, k. Changes in the dimensionless quantity α/k (referred to below and in the figures simply as "attenuation") can then be compared in magnitude to the concurrent changes in $\Delta f/f_o$ (provided κ is near unity) to estimate their relative "significance" in a qualitative sense.[1b,35]

Results and Discussion

Selectivity and DIMP Multilayer Formation on the $(COO^-)_2/Cu^{2+}$-Terminated Surface. Figure 2A shows frequency shift ($\Delta f/f_o$ from eq 1) as a function of vapor-phase concentration for six different organic analytes, as well as water, interacting with a SAW device covered by a $(COO^-)_2/Cu^{2+}$-terminated monolayer film. The organomercaptan SAM was allowed to form for 180 h on a room-temperature-deposited Au surface. For

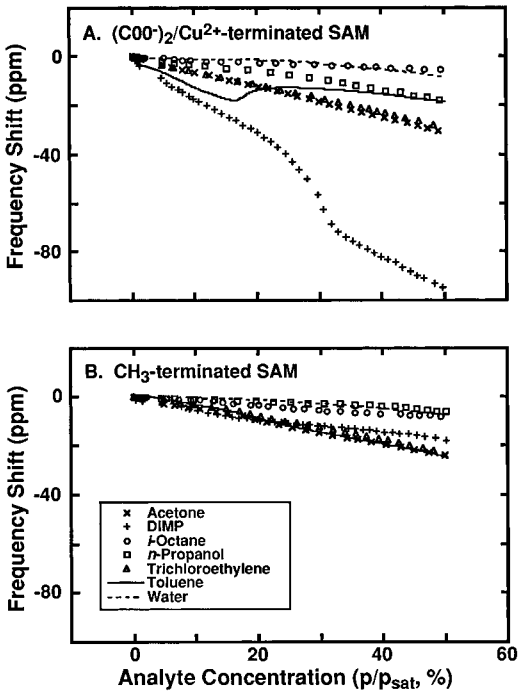

Figure 2. Adsorption isotherms for a SAW device, covered with either a (A) $(COO^-)_2/Cu^{2+}$- or a (B) CH_3-terminated monolayer film, exposed to six different organic analytes and water. Each isotherm was obtained over the course of 2 h. The same scales are used in both parts of Figure 2 to directly compare the response of the two monolayer films. In (A), the equivalent coverage for the DIMP analyte at 50% of saturation is about 17 layers. The next-highest coverage corresponds to approximately nine layers for the acetone analyte.

clarity, only a small percentage of the recorded data points are plotted; note that negative frequency shifts correspond to increased mass loading (eq 1). The data in Figure 2A indicate that multilayers form (based on molar volumes from the bulk liquids) at $p/p_{sat} = 0.5$ for all the analytes examined but isooctane. The *number of multilayers* that adsorb gives a qualitative indication of the "range" of the interaction. It is thus interesting to note that the frequency shift for DIMP at $p/p_{sat} = 0.5$ is consistent with the adsorption of approximately 17 layers of DIMP, assuming the layers have the density of the bulk liquid and that the SAW response is entirely due to mass loading. This value is significantly larger than the next-highest equivalent mass coverage for an analyte at $p/p_{sat} = 0.5$, about nine layers for acetone; the coverage of water is about three layers at the same p/p_{sat} value. Apparently, DIMP is the most amenable of the species examined to multilayer formation. It is noteworthy that, for all of these analytes, this multilayer formation is a fully reversible process: when the N_2-entrained-analyte-vapor stream is replaced by a pure N_2 stream, the SAW frequency eventually returns to a relative frequency shift of zero.

As discussed in more detail below, we find that changing either the solution-phase formation time of the SAM or the grain size of the Au surface supporting the SAM can dramatically influence the extent of multilayer formation. These results provide indirect evidence that analyte multilayer formation is a result of molecular ordering induced by the SAM, the ordering of the SAM being a function of the conditions under which it is formed.

The adsorption of the various analytes of Figure 2A also results in reversible, concentration-dependent attenuation of the acoustic wave (not shown), the magnitude of which is in approximate proportion to the frequency shift. Attenuation of the acoustic wave is often related to

(33) Ashcroft, N. W.; Mermin, N. D. *Solid State Physics*; Saunders College, 1976; Chapter 4, p. 63.
(34) Golan, Y.; Margulis, L.; Rubinstein, I. *Surf. Sci.* **1992**, *264*, 312.
(35) Ricco, A. J.; Martin, S. J. *Thin Solid Films* **1992**, *206*, 94.
(36) Martin, S. J.; Ricco, A. J.; Ginley, D. S.; Zipperian, T. E. *IEEE Trans. UFFC*, **1987**, *UFFC-34*, 142.
(37) The average grain size of the Au SAW transducers, which were prepared over a Ti adhesion layer, was initially 60 nm (approximately the same as the ones evaporated at room temperature with no adhesion layer). Thermal annealing the devices up to 300 °C caused the grain size to increase by no more than 35%.

changes in the mechanical properties of surface layers;[30,31] because such mechanical interactions also influence SAW velocity, the equivalent mass coverage calculated with eq 1 may not be completely accurate.[38] We do not expect that correction for this effect would change the chemical selectivity trends discussed in detail below because all the analytes cause attenuation in approximate proportion to the size of the response. Corroborating ellipsometric data suggest the frequency shift may be an overestimate of the multilayer coverage by a factor of no more than 2,[39] and polarization-modulation FTIR data also indicate the formation of multilayer films for this system.[40]

The Methyl-Terminated Surface. In contrast to the results for the $(COO^-)_2/Cu^{2+}$-terminated surface, Figure 2B shows SAW results (adsorption isotherms) for the same group of analytes interacting with a CH_3-terminated SAM. In this case, the SAM was allowed to form for 84 h on a room-temperature-deposited Au surface. The vapor/solid interface of the CH_3-terminated monolayer is not expected to be appreciably affected using a shorter SAM formation time because the chemical nature of this film can be attributed solely to van der Waals interactions (as opposed to ordering associated with hydrogen bonding (H bonding) of the carboxylic acid groups in the acid-terminated SAM).[22b] As illustrated in Figure 2B, there is clearly no preference for the organophosphonate using this chemically insensitive interface. The same scales are used in both parts of Figure 2 to directly compare the response of the two monolayer films. Nonspecific interactions between the analyte and the monolayer film (i.e., van der Waals) as well as specific interactions between adsorbing analyte molecules account for the relative differences in adsorbed mass.

Chemical Selectivity. While "raw" frequency changes are sometimes used as an indication of selectivity, such data are necessarily biased in favor of analytes with higher molecular weight: for a given surface coverage of an analyte, expressed as number of molecules/area, the higher molecular weight species causes a proportionately larger frequency shift. To make a more objective assessment of the extent of selectivity, we normalized the data of parts A and B of Figure 2 for analyte molecular weight and replotted the isotherms in parts A and B of Figure 3, respectively. Expressed as the number of moles adsorbed/area, the adsorption isotherms in Figure 3A reveal preferential response to DIMP and acetone relative to other common organic solvents. We initially expected that these two preferred analytes should have moderately strong interactions with the $(COO^-)_2/Cu^{2+}$-terminated surface because of their available oxygen lone pairs; the coordinated Cu^{2+} is a Lewis acid and these two analytes are Lewis bases. Only the DIMP analyte, however, shows an appreciable amount of specific binding with this composite monolayer film when the results for the methyl-terminated SAM are taken into account (see discussion below). Water is next in extent of coverage; the shape of the water isotherm, which rises fairly steeply above $p/p_{sat} = 0.3$, is probably influenced by water's ability to form H-bonded networks with itself. Note that neither polarity nor H-bonding capability alone can explain the selectivity trend. Next in order of selectivity are 1-propanol, trichloroethylene, and toluene. Propanol forms H bonds, TCE can H bond weakly and might also be expected to have mild interactions between its Cl substituents and the Cu^{2+}, and the response to toluene is anomalous, showing

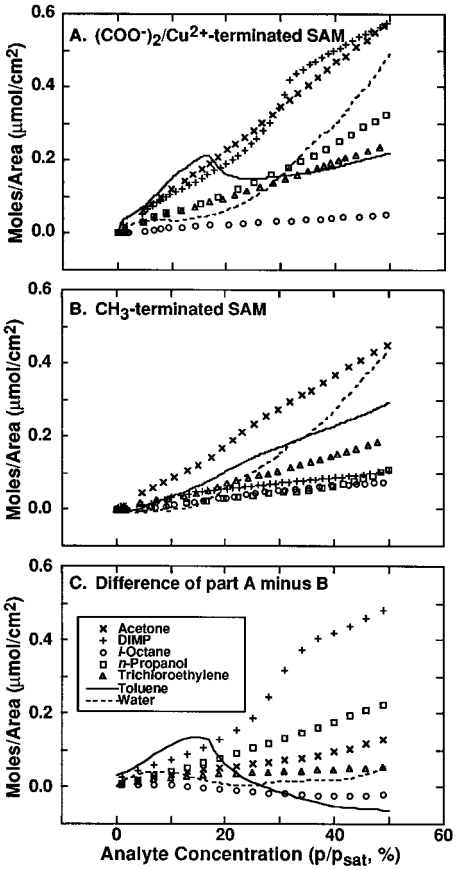

Figure 3. Adsorption isotherms of Figure 2 normalized for the molecular weight. The scales are identical in parts (A) and (B) to facilitate direct comparison between the two chemically-distinct SAM films. As discussed in the text, the degree of specificity of adsorbate/SAM interactions is most readily ascertained by comparing the number of moles adsorbed/area for two chemically distinct monolayer films, which is facilitated by the difference isotherms from part A minus part B, shown in (C).

significant nonmonotonicity near $p/p_{sat} = 0.2$. Such behavior is typically a consequence of changes in the (visco)elastic properties of a thin film;[1b,31] a small but measurable peak in the attenuation was also observed with the sigmoidal deflection of the frequency shift, as is often the case for such effects. The last-place finish by isooctane, the least polar of all the analytes examined, is no surprise.

The degree of specificity of adsorbate/SAM interactions is most readily ascertained by comparing the number of moles adsorbed/area for the CH_3- and $(COO^-)_2/Cu^{2+}$-terminated monolayer films. To facilitate this comparison, the differences between the isotherms of parts A and B of Figure 3 are plotted in Figure 3C. The response to DIMP is nearly six times larger at $p/p_{sat} = 0.5$ for the $(COO^-)_2/Cu^{2+}$-terminated interface than the CH_3-terminated interface. The data clearly indicate a high degree of molecular specificity between DIMP and the $(COO^-)_2/Cu^{2+}$-terminated SAM (though we expect such specificity to apply to organophosphonates as a class, not to DIMP alone), further supporting our hypothesis regarding adsorbate ordering induced by the composite monolayer film. The small interaction measured between the DIMP analyte and the CH_3-terminated SAM is most likely due to van der Waals interactions. In marked contrast, the similarity in magnitude and shape of the response for both acetone and water adsorbed on the two different SAM surfaces (note the very small difference curve for these species in Figure 3C) suggests that their adsorption is

(38) Grate, J. W.; Klusty, M.; McGill, R. A.; Abraham, M. H.; Whting, G.; Andonian-Haftvan, J. *Anal. Chem.* **1992**, *64*, 610.
(39) Thomas, R. C.; et al. Manuscript in preparation.
(40) Yang, H. C.; McEllistrem, L.; Ricco, A. J.; Crooks, R. M. Manuscript in preparation.

dominated by interactions that are not a specific consequence of the SAM terminal group chemistry. The tendency of H_2O to form H-bonded networks with itself probably explains its relatively large response. *A priori*, a similar effect would not be expected for acetone, which has no H-bonding protons. However, the acetone was not rigorously dried, so the entrained vapor undoubtedly contains a small amount of water, which we suspect may participate in the formation of a H-bonded network, promoting multilayer adsorption. A second possibility involves grain-boundary adsorption: defects in the SAM necessarily occur at Au grain boundaries, perhaps exposing sulfur head groups and/or forming "cracks" that are attractive to molecules with the appropriate size, shape, and chemical properties. To first order, the data indicate that any such effect is independent of the SAM tail group.

The most important conclusion to be drawn from comparison of parts A and B of Figure 3 is that a pair of chemically sensitive SAW devices, one functionalized with the $(COO^-)_2/Cu^{2+}$- and the other with the CH_3-terminated monolayer film, readily distinguishes chemically specific from nonspecific adsorption of analytes. This conclusion is further illustrated by comparison of the relative responses measured for 1-propanol and trichloroethylene (see Figure 3C): the SAW device with the $(COO^-)_2/Cu^{2+}$-terminated SAM shows about three times the response for propanol as the methyl-terminated SAM, an indication of specific interaction between the propanol (and probably alcohols as a class) and the more polar monolayer film. For TCE, the response is only about 30% larger for the $(COO^-)_2/Cu^{2+}$-terminated film, indicating a minor role for specific interactions. Only two of the species examined actually show a larger surface coverage at $p/p_{sat} = 0.5$ for the methyl-terminated surface than for the $(COO^-)_2/Cu^{2+}$ surface: isooctane and toluene, the least polar of the analytes. In the case of toluene, the precise extent of the difference is clouded by the partially non-mass-related response observed in Figure 3A. For isooctane, though the response is small compared to the other analytes, it is nonetheless about 60% greater for the CH_3-terminated surface, in accord with the very similar chemical nature of the surface and the analyte in this case.

Dependence on SAM Formation Time. Figure 4 shows a series of DIMP adsorption isotherms obtained from SAW devices covered by $(COO^-)_2/Cu^{2+}$-terminated monolayer films that were assembled by adsorption from ethanolic solution for times of 36, 84, or 180 h. The polycrystalline Au films upon which the SAMs were formed were evaporated onto room-temperature quartz substrates, with a resultant average Au grain size of 50 nm (see Figure 6A and discussion in the next section). The binding affinity of this selective coating for DIMP increases dramatically as the MUA monolayer film is allowed to form for longer periods of time (Figure 4A). While our evidence is circumstantial, we believe that long adsorption times allow (re)organization of the SAM to provide a lower energy structure and an orientation of the $(COO^-)_2/Cu^{2+}$-terminated layer that is more favorable for inducing ordering in adsorbed DIMP.

To complement the frequency-shift data of Figure 4A, Figure 4B shows the corresponding SAW attenuation data obtained during the same adsorption isotherms. Appreciable attenuation of the acoustic wave occurs only for the MUA monolayer film prepared for 180 h, a definite indication that this film differs in its structural/mechanical properties from the SAMs prepared for shorter adsorption times.

Long adsorption times are likely to affect the structural properties of the alkane portion of the MUA monolayer, which could also affect the orientation of the carboxylate

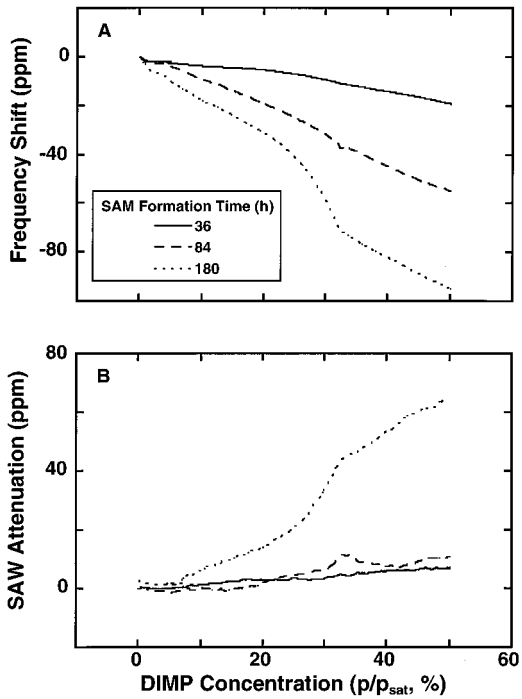

Figure 4. DIMP adsorption isotherms for SAW devices covered by $(COO^-)_2/Cu^{2+}$-terminated monolayer films. The MUA SAMs were fabricated using solution-phase adsorption times of 36, 84, or 180 h. The frequency shift as a function of concentration (A) increases with the solution-phase SAM formation time. Enhanced sensitivity results from structural ordering effects at the vapor−solid interface of the composite monolayer film. (B) Corresponding attenuation data.

end groups and hence the Cu^{2+} they coordinate. Previous reports have shown that the alkane portion of MUA monolayer films are in a "liquid-like" environment after solution-phase adsorption times ranging from 10 to 36 h.[22b,41] The hydrocarbon chain probably becomes more "crystalline" after longer adsorption times since it is known that completion of the self-assembly process can take several days.[28] Although structural defects measured on a nanometer scale in methyl-terminated films formed for 24−48 h can be dramatically improved by thermal annealing,[26,27,42] the monolayer as a whole becomes much more porous; that is, one type of defect is replaced by another. The long adsorption times used in the present study can be likened to a long-duration, low-temperature anneal, which avoids the difficulty of increasing porosity by keeping the films in a solution of thiol during formation.

In addition to orientation effects, carboxylic acid-terminated SAM films are known to undergo extensive intramonolayer hydrogen bonding.[22c,39,43] The 180-h adsorption time may allow the MUA film to form a more extended H-bonding structure throughout the monolayer, leading to a $(COO^-)_2/Cu^{2+}$ interface more favorable to inducing ordering in adsorbed DIMP multilayers. Although our SAW data agree with this line of reasoning, additional spectroscopic measurements (surface infrared) are underway to confirm this hypothesis.[40]

To learn if the adsorption−time effects discussed above are associated with MUA multilayer formation, ellipsometry was carried out directly on the Au/SAM-modified SAW

(41) Smith, E. L.; Alves, C. A.; Anderegg, J. W.; Porter, M. D. *Langmuir* **1992**, *8*, 2707.
(42) Camillone, N., III; Eisenberger, P.; Leung, T. Y. B.; Schwartz, P.; Scoles, G.; Poirier, G. E.; Tarlov, M. J. *J. Phys. Chem.* **1994**, *101*, 11031.
(43) Nuzzo, R. G.; Dubois, L. H.; Allara, D. L. *J. Am. Chem. Soc.* **1990**, *112*, 558.

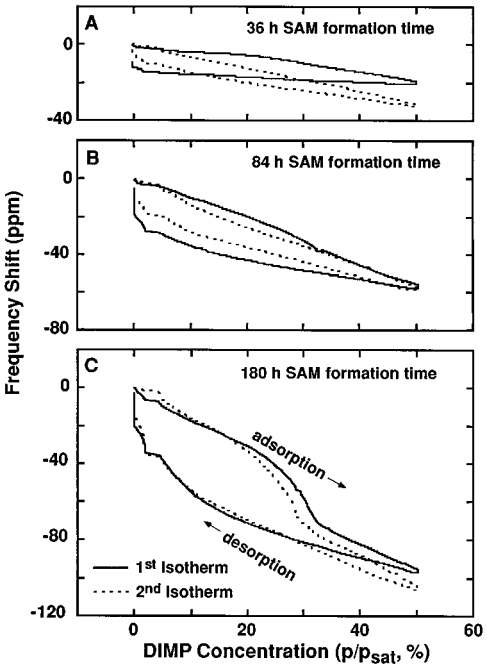

Figure 5. Full adsorption/desorption isotherms, in terms of frequency shift versus vapor-phase DIMP concentration, for $(COO^-)_2/Cu^{2+}$-terminated monolayer films prepared for adsorption times of (A) 36, (B) 84, or (C) 180 h. The Au films were deposited at room temperature. For each composite SAM film, one DIMP adsorption/desorption isotherm was obtained before (solid lines) and after (dashed lines) similar isotherms of the other 6 analytes listed in Figure 2. The data suggest that resistance to aging improves with increasing SAM formation time. These "stability effects" were also observed for composite SAM films prepared on Au surfaces having different grain sizes.

device surface.[39] These measurements indicate that the thickness of all the composite SAMs for which SAW data are shown in Figure 4 is 1.9 ± 0.5 nm, in agreement with previous measurements of MUA films.[44,45] While these measurements are not accurate enough to indicate subtle thickness differences, they do confirm that only a single monolayer of MUA forms, regardless of the solution-phase adsorption time.

The time of formation of the $(COO^-)_2/Cu^{2+}$-terminated monolayer films also affects the "aging" characteristics of these interfaces. Figure 5 shows both adsorption and desorption branches of DIMP isotherms for $(COO^-)_2/Cu^{2+}$-terminated monolayer films prepared on 50-nm grain-size Au films. As in the data of Figure 4, the formation times used to fabricate the SAMs from ethanolic solution were 36, 84, or 180 h. Each complete isotherm was obtained over the course of 4 h. For each composite SAM, the first isotherm (solid line) was obtained immediately after the film was prepared, and the second one (dashed line) after it had been exposed to the other organic analytes listed in Figure 2. There is significant hysteresis between the adsorption and desorption branches of the isotherms, likely an indication that the $(COO^-)_2/Cu^{2+}$-terminated surface and the DIMP analyte do not attain equilibrium on the time scale of the isotherm.[46] While the magnitude of the hysteresis, particularly at low concentrations, becomes greater as the SAM formation time increases, note that the difference between the first and second isotherms (solid vs dashed lines) is relatively much smaller for the SAMs with the longest formation time. This effect is also observed for composite monolayer films prepared on Au surfaces having larger grain sizes. Our results are fully consistent with the hypothesis of enhanced SAM-induced analyte ordering: more hysteresis is observed using SAMs prepared for long formation times because the DIMP analyte binds more strongly on the better organized surface, which makes desorption more difficult.

Since the two isotherms were obtained before and after exposure to a series of organic analytes, we believe the differences arise from solvent effects on the nature of the $(COO^-)_2/Cu^{2+}$ interface—in particular, solvent-induced relaxation of the film to a lower energy structure (the solvents in this case being at least some of the various analytes, listed in Figure 2, to which the film was exposed). The smaller difference between the initial and final DIMP isotherms shown in Figure 5C suggests that the film prepared for the longest adsorption time is in the most stable conformation of the three, in agreement with the conclusions drawn above from the data of Figure 4. Note, however, that this solvent-induced relaxation is very minor compared to the effect of long-duration deposition of the SAM films; this is clear because we have dosed these films repeatedly with many solvents for many hours and observed no evidence that room-temperature solvent vapor exposure will ever convert the behavior of the films represented in parts A and B of Figure 5 into that of the 180-h-deposited film of Figure 5C.

Finally, we note that the large hysteresis recorded at low partial pressures for the most stable configuration of the monolayer (Figure 5C, $p/p_{sat} = 0$ to 0.3) is also in accord with our hypothesis regarding ordering. The reason is that well-ordered DIMP multilayers, once formed, may be relatively slow to desorb, a consequence of the additional stability afforded by their organized structure.

Gold Grain-Size Effects. Figure 6 shows 1 μm × 1 μm atomic force microscopy (AFM) images that illustrate the variable, controlled grain sizes of the Au surfaces used to support the composite monolayer films. All of the images were obtained directly on the SAW device surface following SAW adsorption measurements. The same height scale (30 nm) was used to facilitate direct comparison of the images. The average grain sizes estimated from the AFM images shown in parts A–C of Figure 6 are approximately 50, 80, and 240 nm, respectively. The corresponding root mean square surface roughness for these Au films estimated from the AFM data is 1.2, 1.3, and 1.1 nm. We have obtained similar results for both the grain size and surface roughness by analyzing 5 μm × 5 μm AFM images. Since the AFM images are not resolved on an atomic scale, we have also electrochemically measured the surface roughness factor of bare Au films. Our results, which are intended only to indicate relative differences in surface roughness (as opposed to absolute area measurements) show that the surface roughness factor varies by only 11% for the Au films used in these studies, which have grain sizes between 50 and 240 nm.[39] The important result from the AFM and electrochemical

(44) Chidsey, C. E. D.; Loiacono, D. N. *Langmuir* **1990**, *6*, 682.

(45) Ellipsometric measurements were done using a Gaertner Model L2W26D.488 ellipsometer with a He–Ne laser at a 70% angle of incidence and a 45% azimuth of the quarter-wave compensator. Film thicknesses were calculated by using a real refractive index of 1.45, the complex refractive index of a similarly prepared naked Au substrate, and an algorithm developed at Sandia National Laboratories (Tardy, H. L. ELLIPSE User's Manual and Program Reference; Report No. 89-0008; Sandia National Laboratories: Albuquerque, NM, 1989).

(46) There are instances, notably when the adsorption substrate is porous, in which complete thermodynamic equilibrium can be maintained throughout an isotherm, even though the adsorption and desorption branches differ significantly. This is a consequence of the different radii of curvature that pertain if the meniscus of layers of adsorbate coating the walls of pores is cylindrical (during filling) or spherical (during emptying): Adamson, A. W. *Physical Chemistry of Surfaces*, 4th ed.; John Wiley & Sons: New York, 1982; pp 584–589. We do not believe there is sufficient porosity in the present instance to support this phenomenon, but we cannot unequivocally rule it out.

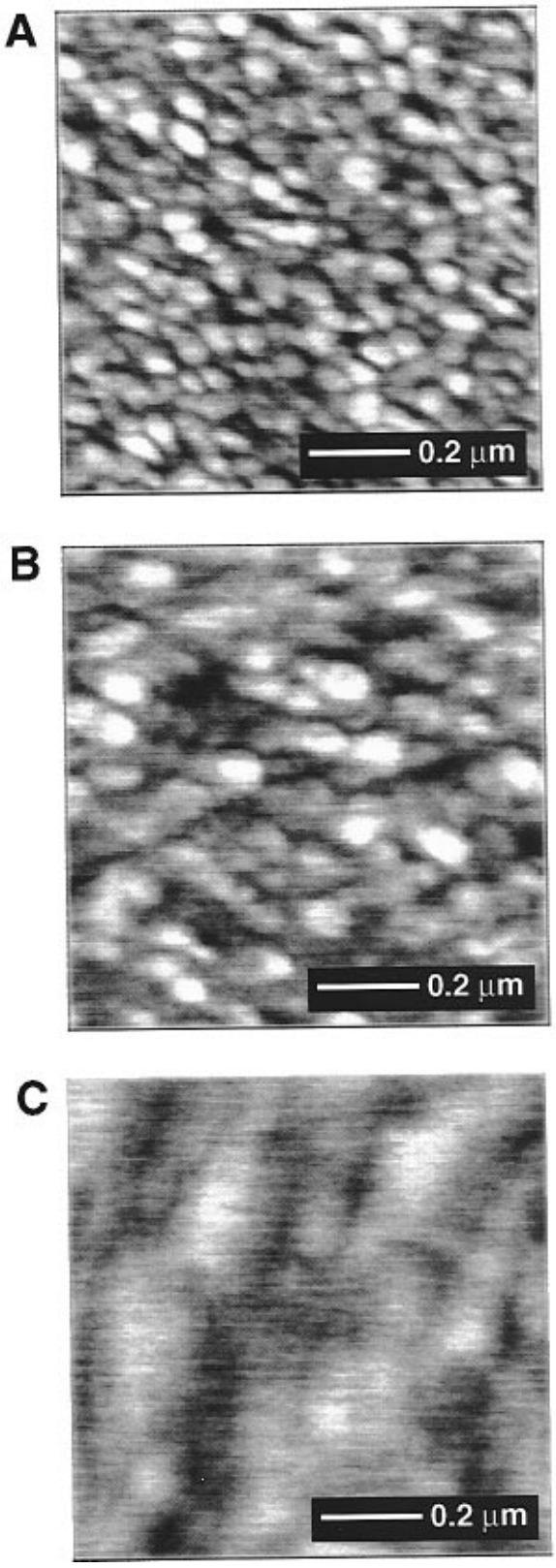

Figure 6. Constant repulsive-force images of 100 nm thick Au films evaporated onto ST-quartz SAW devices. The Au films were electron-beam evaporated at (A) room temperature, (B) 100 °C followed by a 2 h anneal at 150 °C, and (C) 100 °C followed by a 2 h anneal at 250 °C. The average grain size and surface roughness, respectively, for the different deposition conditions were (A) 50 and 1.2 nm, (B) 80 and 1.3 nm, and (C) 240 and 1.1 nm.

measurements is that the average grain size varies by about a factor of 5, while the surface roughness is approximately the same for the different Au films.

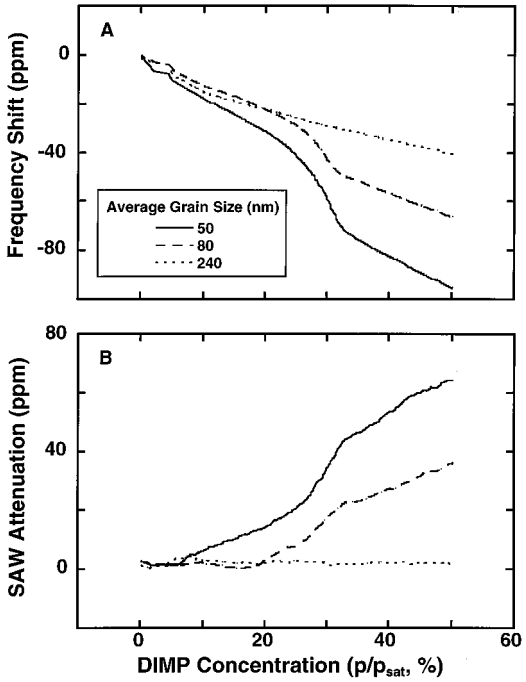

Figure 7. DIMP adsorption isotherms for composite monolayer films prepared on the Au surfaces having the variable grain sizes shown in Figure 6. (A) Frequency shift and (B) SAW attenuation versus the vapor-phase concentration of DIMP illustrate that sensitivity of SAW devices with composite SAMs prepared on Au films increases as grain size decreases. Although the MUA films were formed for 180 h in this case, similar effects are observed for shorter formation times.

Figure 7 shows DIMP adsorption isotherms for $(COO^-)_2/Cu^{2+}$-terminated SAMs prepared on the variable-grain-size Au surfaces of Figure 6. The Au surfaces shown in parts A−C of Figure 6 produced the SAW data shown in Figure 7 by the solid, dashed, and dotted lines, respectively. Clearly, as the grain size of the Au film *decreases*, there is a significant *increase* in the extent of adsorption of DIMP at a given p/p_{sat}. Electrochemical measurements indicate that surface roughness is *not* the dominant factor in these results: while the roughness changes by about 10%, the SAW response varies by a factor of 2.5 at $p/p_{sat} = 0.5$ from the largest to smallest grain size. Furthermore, thermally deposited Au films have predominantly (111) crystallite orientation,[34] and this is not altered by annealing, so the total coverage of the MUA SAMs for the three grain sizes should be very similar. Rather, we postulate that the grain-size-dependent extent of adsorption in Figure 7 results from grain-size-induced changes in the surface properties of the $(COO^-)_2/Cu^{2+}$-terminated SAMs, changes that are related to the nature and extent of ordering, in analogy to the adsorption-time-dependent data presented above.

The extent of the attenuation of the acoustic wave also shows an inverse relationship to Au grain size (Figure 7B), further supporting the notion that grain size has a strong influence on the structural properties of the SAM and its consequent interactions with adsorbed analyte. While direct interactions between adsorbed analyte and Au grain boundaries might seem a plausible explanation for the results of Figure 7B, similar results are *not* obtained for methyl-terminated SAMs prepared on Au surfaces having the same set of different grain sizes: attenuation shows essentially no grain-size dependence.

The data of Figure 7 were obtained from MUA SAMs formed for 180 h *via* solution-phase adsorption. While we have observed similar grain-size effects when the MUA film formation time is 36 or 84 h, the effect is most

pronounced for the 180-h formation time. Furthermore, our results show not only that the formation of MUA SAMs for 180 h on different grain sizes is reproducible but there is also less variation in samples formed on smaller grains compared to larger ones. Experiments are currently in progress to quantitatively determine the reproducibly of preparing a more statistically significant set of composite SAM films for long formation times on small grains.

Summary and Conclusions

We have studied the selectivity, sensitivity, and reproducibility of SAW sensors covered by $(COO^-)_2/Cu^{2+}$-terminated monolayers by examining the response of SAM films formed from the solution phase for adsorption times ranging from 36 to 180 h. These SAMs were prepared on thin-film Au surfaces having variable, controlled grain size.

Our results show that a pair of SAM-functionalized SAW sensors, one bearing a methyl- and the other a $(COO^-)_2/Cu^{2+}$-terminated monolayer, allow clear distinction to be drawn between chemically specific and nonspecific adsorption of analytes. The results further show that the composite SAM films (1) preferentially adsorb particular classes of organic analytes in a manner that follows from simple concepts such as Lewis acid/base, H-bonding, and polar vs nonpolar interactions, (2) readily and reversibly adsorb the equivalent of 10−20 layers of some analytes at $p/p_{sat} = 0.5$, (3) adsorb a greater quantity of DIMP at a given partial pressure for longer solution-phase formation times of the organomercaptan monolayer, (4) display the least organic analyte-induced aging (ordering/relaxation) effect when the SAM films have been formed for the longest solution-phase adsorption times, and (5) adsorb a greater quantity of DIMP at a given partial pressure as the grain size of the supporting Au film decreases. While result 1 is straightforward and to be expected, we believe results 2−5 are consequences of the extent and nature of the ordering of the SAM and its outer surface: the ordering affects the thermodynamics of adsorption of multilayers. Although it must be acknowledged that this hypothesis is speculative, we can postulate no other thermodynamically viable explanation, given the absence of surface porosity, for the equilibrium formation of 10−20 layer thick films of adsorbate at p/p_{sat} values of only 0.5, nor can we offer another plausible explanation for the hysteresis results of Figure 5. "Long-range" chemical interactions extending through so many layers of adsorbate are simply unreasonable. Result 3 in particular points to the outer $(COO^-)_2/Cu^{2+}$ SAM surface becoming better suited to inducing ordering in adsorbed DIMP multilayers as more stable SAM conformations are attained. The results from these measurements are an important step toward reliably fabricating chemical sensor arrays that respond to organic analytes with controlled class and/or molecular specificity.

Acknowledgment. R.C.T. and A.J.R. acknowledge the excellent technical assistance of Al Staton and Mary-Anne Mitchell. The authors also acknowledge Dan Dermody (Texas A&M University) for his help setting up the SAW/Ellipsometry experiments. The work performed at Sandia National Laboratories was supported by the U.S. DOE under Contract DE-ACO4-94AL85000. H.C.Y. and R.M.C. acknowledge support by the National Science Foundation (CHE-9313331).

LA950498W